Interplay between hybridization gaps and antiferromagnetic gap in the hole-doped Kondo semiconductor $Ce(Os_{1-y}Re_y)_2Al_{10}$

Jo Kawabata[1], Toshikazu Ekino[2], Yoshihiro Yamada[1],

Akira Sugimoto[2], Yuji Muro[3] and Toshiro Takabatake[1, 4,*]

[1] Department of Quantum Matter, Graduate School of Advanced Sciences of Matter, Hiroshima University, Higashi-Hiroshima 739-8530, Japan

[2] Graduate School of Integrated Arts and Sciences, Hiroshima University, Higashi-Hiroshima 739-8526, Japan

[3] Liberal Arts and Sciences, Faculty of Engineering, Toyama Prefectural University, Imizu, Toyama 939-0398, Japan

[4] Institute for Advanced Materials Research, Hiroshima University, Higashi-Hiroshima 739-8521, Japan

E-mail: takaba@hiroshima-u.ac.jp

Abstract. The Kondo semiconductor $CeOs_2Al_{10}$ undergoes an antiferromagnetic (AFM) order at an unexpectedly high temperature 28.5 K. We have performed break junction tunneling measurements for the hole-doped system $Ce(Os_{1-y}Re_y)_2Al_{10}$ ($y \leq 0.1$). The tunneling spectrum dI/dV for $y = 0$ displays successive openings of a hybridization gap V_1, an AFM gap V_{AF} and another hybridization gap V_2 in the density of states (DOS). On cooling from 36 K to T_N, both the gap value V_1 and the DOS at the Fermi level, E_F, decrease by 8% of the values at 36 K. This fact indicates that the development of short-range magnetic correlations reduces the *c-f* hybridization gap. For $y = 0.02$, a peak appears in dI/dV at $V = 0$ concurrently with the disappearance of V_2. With increasing y further, the in-gap states develop at E_F, in good agreement with the increase in the Sommerfeld coefficient of the heat capacity. Thereby, T_N, V_1 and V_{AF} decrease and disappear at $y = 0.05$. These facts provide compelling evidence that the presence of V_1 is necessary for the AFM order in $CeOs_2Al_{10}$.

1. Introduction

A family of cerium-based compounds CeT_2Al_{10} (T = Fe, Os and Ru) belongs to Kondo semiconductors. For example, the resistivity $\rho(T)$ in the Os compound shows a thermal activation-type temperature dependence at $30 < T < 80$ K. Nevertheless, this compound undergoes an antiferromagnetic (AFM) transition at rather high Néel temperature T_N of 28.5 K [1,2]. It has remained a mystery that the T_N with a small magnetic moment 0.3 μ_B/Ce is higher than T_N = 18 K for the Gd counterpart with 7 μ_B/Gd [3]. Below T_N, the slope of $\rho(T)$ increases abruptly, most likely by the formation of a superzone gap. The analysis of anisotropic magnetic susceptibility and the x-ray absorption spectra for single crystals

determined the crystal-field ground state to be a Kramer's doublet dominated by $|J_z> = |\pm 3/2>$, where $|J_z>$ is the *c*-axis component of the total angular momentum $J = 5/2$ [4].

The break junction tunneling spectroscopy (BJTS) is a powerful method to detect fine changes in the density of states (DOS) caused by AFM and charge-density-wave (CDW) transitions. The BJTS uses a crack prepared in a sample as an insulating barrier for the semiconductor-insulator-semiconductor (SIS) junction. Cracking the sample in a liquid-helium atmosphere provides a clean interface without any contamination and oxidation of reactive Ce based compounds. Furthermore, the SIS junction is not affected by the Seebeck effect so that symmetric tunneling spectra are observed [5]. The BJTS for the antiferromagnet $Ce(Fe_{0.95}Co_{0.05})_2$ showed peaks at $V = \pm 10$ mV below $T_N = 45$ K due to a superzone gap opening in the DOS at E_F [6]. The CDW gap in $CeTe_2$ was found to decrease when a short-range ferromagnetic order develops at low temperatures. This observation in $CeTe_2$ revealed the interplay between the CDW and magnetic order [7].

Recently, BJTS measurements for CeT_2Al_{10} (T = Fe, Os) have revealed openings of two gaps (Δ_1 = 150 meV, Δ_2 = 38 meV) in $CeFe_2Al_{10}$ and three gaps (Δ_1 = 100 meV, Δ_{AF} = 50 meV, Δ_2 = 25 meV) in $CeOs_2Al_{10}$ [8]. In the latter, the AFM gap Δ_{AF} develops below T_N. We pointed out that Δ_1 and Δ_2 are proportional to the Kondo temperature T_K, and the ratio Δ_1/Δ_2 is approximately 4 for the two compounds with T = Fe and Os. These relations, $\Delta \propto T_K$ and $\Delta_1/\Delta_2 = 4$, agree with those for the double *c-f* hybridization gaps calculated with the periodic Anderson model for a crystal-field ground state consisting of $|J_z> = |\pm 3/2>$ [9].

The 5*d* hole and electron doping effects in $Ce(Os_{1-y}Re_y)_2Al_{10}$ and $Ce(Os_{1-x}Ir_x)_2Al_{10}$ systems, respectively, have been studied by the measurements of magnetic properties, optical conductivity and muon spin relaxation (μSR) as well as neutron scattering [10-12]. It is found that the 4*f* state in $CeOs_2Al_{10}$ becomes more itinerant by doping of 5*d* holes, while the 4*f* state is localized by the doping of 5*d* electrons. The semiconducting increase in the $\rho(T)$ below 16 K changes to a metallic behavior at a small level of $y = 0.02$. For $y = 0.1$, $\rho(T)$ exhibits a broad maximum at around 100 K which is a characteristic of valence fluctuating Ce compounds. On the other hand, $\rho(T)$ for the electron doped sample with $x = 0.04$ shows a metallic behavior at low temperatures. For $x = 0.15$, $\rho(T)$ no longer shows the thermal activation behavior above T_N nor the increase below T_N. In both systems doped with 5*d* holes and electrons, the suppression of T_N is well correlated with that of the thermal activation energy Δ/k_B in $\rho(T)$. In contrast, the Sommerfeld coefficient γ in the specific heat increases sharply as x and y are increased. Therefore, we concluded that the presence of the hybridization gap V_1 is necessary for the AFM order in $CeOs_2Al_{10}$. Although the activation energy in $\rho(T)$ gives a crude estimation of the gap width, it does not provide us with the information on the temperature variation of the gap structure. Note that $\rho(T)$ depends on the scattering process and the DOS only at the Fermi level. It is important to observe how the three gaps V_1, V_{AF} and V_2 in $CeOs_2Al_{10}$ are changed by doping the 5*d* holes and electrons.

For this purpose, we have measured the BJTS on the system $Ce(Os_{1-y}Re_y)_2Al_{10}$ ($y \leq 0.1$). We have reported that the sample with $y = 0.02$ undergoes an AFM transition at 23 K, above which $\rho(T)$ still exhibits the activation-type temperature dependence. For $y = 0.05$, however, the AFM transition and the gap Δ/k_B in $\rho(T)$ disappear. Furthermore, $\rho(T)$ in $y = 0.1$ shows a characteristic temperature dependence with a broad maximum around 100 K [10].

2. Sample preparation and break-junction tunneling measurements

For BJTS measurements, polycrystalline samples of $Ce(Os_{1-y}Re_y)_2Al_{10}$ (y = 0, 0.02, 0.05 and 0.1) were prepared by arc melting and subsequent annealing in an evacuated quartz ampoule at 850 ℃ for 7 days [2]. The atomic composition was determined by electron-probe microanalysis, thereby the real compositions of Re were found to agree with the initial ones. In addition, a small amount of impurity phase Os_4Al_{13} has been detected. The midpoint of the jump in the specific heat has been taken as the AFM ordering temperature T_N [10].

The samples were shaped into a plate of 3×2×0.5 mm^3 for BJTS measurements. In order to crack it perpendicularly in the middle, we cut a groove into the surface. The plate was mounted on a flexible substrate, and an adjustable force was applied from its back to make a crack in a liquid-helium chamber. The spectra of *dI/dV*, where *I* and *V* represent the tunneling current and the bias voltage, respectively, have been recorded using a standard lock-in technique by applying *V* along the long axis of the sample [8]. The different thermal expansions between the sample and the substrate made the junction unstable at elevated temperatures. In fact, we could observe the spectra on heating just to 65 K.

3. Experimental results

The tunneling spectra *dI/dV* vs the bias voltage *V* for $Ce(Os_{1-y}Re_y)_2Al_{10}$ (y = 0, 0.02 and 0.05) at 4.4 K are shown in Fig. 1. The spectra are normalized by the values at $V = -400$ mV. The absolute value of *dI/dV* depends on the junction resistance R_J, which is determined by the thickness of insulating barrier [14]. In the high-bias range at $V = -400$ mV, the values of R_J are 20 – 10000 Ω at 4.4 K whose magnitude is much larger than the sample resistance 10 – 50 mΩ measured before breaking. This relation satisfies the condition to measure the voltage drop by the tunneling current in the insulating barrier. By measuring the spectra for many junctions, we confirmed that both the gap structures and the width $V^{P\text{-}P}$ hardly depend on R_J [15]. Such a result is in accordance with a principle of the tunneling spectroscopy.

There are three gap structures in the spectrum for $y = 0$. The peak structures at ± 200, 100 and 50 mV are denoted as V_1, V_{AF} and V_2, respectively, whose values agree with those obtained for single crystals [8]. The peak structures of V_{AF} change to a shoulder in the spectrum for $y = 0.02$, where a peak appears at $V = 0$. This peak structure develops in the spectrum for $y = 0.05$, where the gaps V_1 and V_{AF} disappear. These changes in the spectrum with y indicate that the 5*d* hole doping suppresses the hybridization gaps and induces an in-gap state at E_F. These behaviours are consistent with the gap structures in the DOS calculated on the basis of the periodic Anderson model which takes into a slight dispersion in the *f*-band in the orthorhombic Kondo semiconductors [16].

The temperature dependences of *dI/dV* vs *V* are shown in Fig. 2 for three selected compositions y = 0, 0.02 and 0.1. For $y = 0$, we present the data obtained with the single crystal [8] because the gap structures are clearer than that obtained with the polycrystal. We note that there is little difference in the gap structures between the two. The voltage difference between the shoulders at ±200 mV at 78.5 K is denoted as V_1. On cooling, the shoulders change to peaks. Below T_N, other peaks develop at ±100 mV, whose peak-to-peak voltage is denoted as the AFM gap V_{AF} = 200 mV. On further cooling below 16 K, additional peaks appear at ±50 mV, whose peak-to-peak voltage is denoted as V_2.

In the spectra for $y = 0.02$, the *dI/dV* at 40 K displays shoulders at $V_1/2$. The shoulders change to peaks at 35 K, and transform into shoulders again at $T < 30$ K. On cooling below 27 K ($> T_N = 23$ K), other shoulders appear at $V_{AF}/2$. At low temperatures, the *dI/dV* exhibits a cusp at $V = 0$, which develops

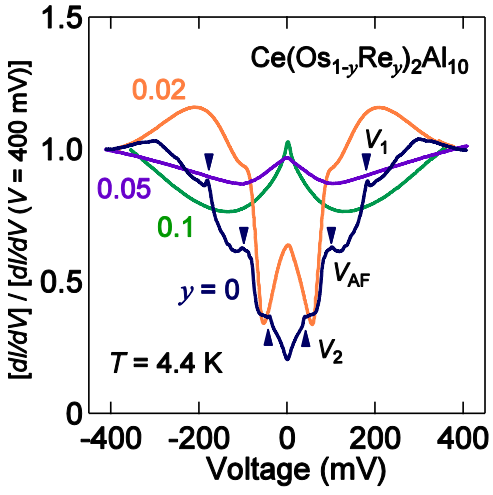

Figure 1. Tunneling conductance spectra *dI/dV* vs the bias voltage *V* normalized by the values at $V = -400$ mV for $Ce(Os_{1-y}Re_y)_2Al_{10}$ (y = 0, 0.02 and 0.05) at 4.4 K. The arrows on the spectrum for $y = 0$ indicate the structures V_1, V_{AF} and V_2, respectively.

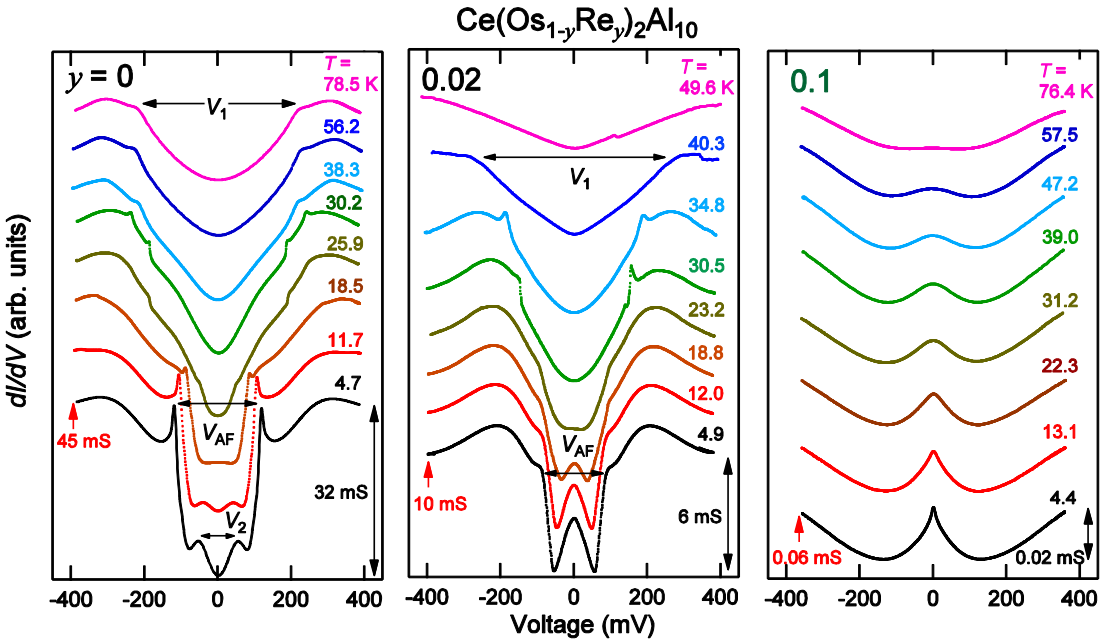

Figure 2. Temperature dependences of the tunneling conductance dI/dV vs V measured for break junctions of $Ce(Os_{1-y}Re_y)_2Al_{10}$. The spectra are shifted vertically for clarity. The widths between shoulders in the spectra are denoted as V_1, V_{AF} and V_2, respectively (see text).

into a peak on cooling. The spectra for $y = 0.1$ is characterized by one cusp at $V = 0$. The development of a cusp at $V = 0$ is a characteristic of a metallic heavy fermion state [17]. It indicates that the $4f$ state in $CeOs_2Al_{10}$ becomes more itinerant by $5d$ hole doping. With increasing y, in fact, the behavior of $\rho(T)$ changes from the Kondo semiconducting one to that for the valence fluctuating Ce compounds [10].

The temperature dependences of the gap widths $V^{P\text{-}P}$ (= V_1, V_{AF} and V_2) are plotted in Fig. 3(a). For $y = 0$, the black and blue data are obtained with a single crystal and a polycrystal, respectively, whose temperature variations are essentially same. The gap width V_1 for $y = 0$ decreases from 430 to 400 mV at around 36 K, which is still above $T_N = 28.5$ K. We recall that the CDW-like charge gap develops in $CeOs_2Al_{10}$ on cooling below 36 K [18]. Similarly for $y = 0.02$, V_1 decreases on cooling from 50 to 27 K ($> T_N = 23$ K). It is reminiscent of the CDW gap in $CeTe_2$ which decreases on cooling below 6.1 K, where a short-range ferromagnetic order develops [6]. By analogy, the reduction in V_1 occurring above T_N in $Ce(Os_{1-y}Re_y)_2Al_{10}$ ($y = 0$, 0.02) may be attributed to the onset of a short-range magnetic correlation. The gap V_{AF} for $y = 0$ increases gradually below T_N, whereas that for $y = 0.02$ seems to appear suddenly at 27 K. The gap V_2 for $y = 0$ appears below 16 K, but corresponding anomaly is absent for $y = 0.02$.

Figure 3(b) displays the temperature dependences of normalized zero bias conductance, $\{NZBC\}^{1/2} = \{[dI/dV\,(V = 0)] / [dI/dV\,(V = -400\text{ mV})]\}^{1/2}$. We note that the NZBC is proportional to the square of the DOS at the Fermi level, $N(E_F)$. The NZBC for $y = 0$ gradually decreases and bends at around 36 K, which occurs simultaneously with the sudden decrease in V_1. It suggests that a part of Fermi surface is lost by the development of the short-range correlation. Besides, the significant change in the Fermi surface on cooling from 36 K manifests in the sharp decrease in the thermopower, which is very sensitive to the energy derivative of quasiparticle density of states at E_F, sharply decreases only along the b-axis [19]. For $y = 0.02$, the decrease in NZBC turns to an increase below 27 K due to the development of in-gap states at E_F. For $y = 0.1$ with no AFM transition, the NZBC increases monotonically on cooling.

Figure 4(a) displays the y dependences of gap widths V_1, V_{AF} and V_2 as well as $\{NZBC\}^{1/2}$. The increase in $\{NZBC\}^{1/2}$ with y is consistent with that in the γ value as shown in Fig. 4(b). The inverse correlation between T_N and γ in Fig. 4(b) indicates that the increase of $N(E_F)$ suppresses the AFM order.

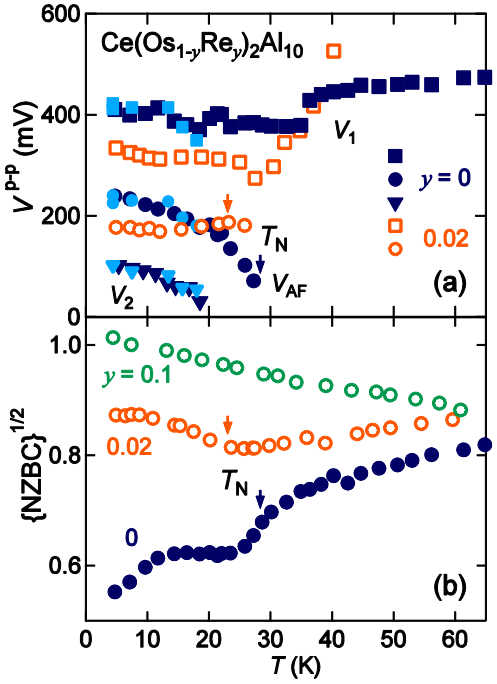

Figure 3. (a) Temperature dependences of gap widths V_1, V_{AF}, V_2 and (b) the square root of normalized zero bias conductance $\{NZBC\}^{1/2} = \{[dI/dV\ (V = 0)] / [dI/dV\ (V = -400\ mV)]\}^{1/2}$ for $Ce(Os_{1-y}Re_y)_2Al_{10}$ (y = 0, 0.02 and 0.1). For y = 0, the data in black and blue are obtained with a single crystal and a polycrystal, respectively. T_N denotes the AFM ordering temperature determined by the specific heat measurements.

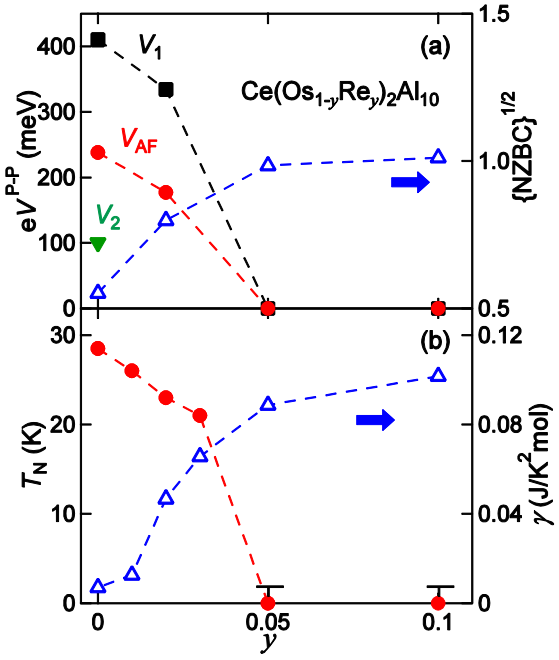

Figure 4. (a) Variations of gap widths V_1, V_{AF}, V_2 and the square root of normalized zero bias conductance $\{NZBC\}^{1/2}$ in the tunneling spectra, and (b) the Néel temperature T_N and the γ value in the specific heat as a function of y in $Ce(Os_{1-y}Re_y)_2Al_{10}$ [20].

Moreover, the T_N and the gap widths V_1 and V_{AF} are largely suppressed at a small hole-doping level y = 0.02, and all disappear at y = 0.05. Therefore, the AFM transition is strongly correlated with the hybridization gap V_1. This relation supports our previous argument that the presence of the hybridization gap V_1 is necessary for the unusual AFM order [10]. Here, let us compare the *c-f* hybridization gap V_1 with the spin gap which was observed by inelastic neutron scattering [12]. The spin gap exists at 11 meV in the undoped sample with y = 0. For y = 0.03, T_N is decreased to 21 K, but the spin gap still exists at the same energy 11meV while the excitation intensity is much reduced. On the other hand, the spin gap disappears in the 5*d* electrons doped systems $Ce(Os_{1.92}Ir_{0.08})_2Al_{10}$ with T_N = 21 K. It is highly required to examine by the BJTS wherever or not the hybridization gap V_1 is correlated with the spin gap.

4. Summary

We have performed the BJTS measurements for the $Ce(Os_{1-y}Re_y)_2Al_{10}$ ($y \leq 0.1$) to study how the two hybridization gaps V_1, V_2 and the AFM gap V_{AF} change by doping of the 5*d* holes in $CeOs_2Al_{10}$ with T_N = 28.5 K. For the undoped sample, both the hybridization gap V_1 and the magnitude of $N(E_F)$ decrease on cooling below 36 K. These reductions occurring above T_N are attributed to a short-range correlation. For y = 0.02, in-gap states develop at E_F with concomitant disappearance of V_2. With increasing y to 0.1,

the in-gap states at E_F develops further. We found a strong correlation between the variations of T_N, V_1 and V_{AF}. Thus, we conclude that the presence of the hybridization gap V_1 above T_N is necessary for the unusual AFM order.

Acknowledgements
We acknowledge valuable discussions with K Umeo, T Onimaru, D T Adroja, S Kimura, T Yokoya, T Yamada and Y Ono. This work was partly supported by KAKENHI Grant Numbers Nos. 26400363, 16H01076 and 15J01007.

References

[1] Nishioka T, Kawamura Y, Takesaka T, Kobayashi R, Kato H, Matsumura M, Kodama K, Matsubayashi K and Uwatoko Y 2009 *J. Phys. Soc. Jpn.* **78** 123705
[2] Muro Y, Kajino J, Umeo K, Nishimoto K, Tamura R and Takabatake T 2010 *Phys. Rev. B* **81** 214401
[3] Muro Y, Kajino J, Onimaru T and Takabatake T 2011 *J. Phys. Soc. Jpn.* **80** SA021
[4] Strigari F *et al*. 2013 *Phys. Rev. B* **87** 125119
[5] Davydov D N, Kambe S, Jansen A G M, Wyder P, Wilson N, Lapertot G and Flouquet J 1997 *Phys. Rev. B* **55** R7299
[6] Fukuda H, Fujii H, Kamura H, Hasegawa Y, Ekino T, Kikugawa N, Suzuki T and Fujita T 2001 *Phys. Rev. B* **63** 054405
[7] Jung M H, Ekino T, Kwon Y S and Takabatake T 2000 *Phys. Rev. B* **63** 035101
[8] Kawabata J, Ekino T, Yamada Y, Sakai Y, Sugimoto A, Muro Y and Takabatake T 2015 *Phys. Rev. B* **92** 201113(R)
[9] Yamada T and Ono Y 2012 *Phys. Rev. B* **85** 165114
[10] Kawabata J, Takabatake T, Umeo K and Muro Y 2014 *Phys. Rev. B* **89** 094404
[11] Khalyavin D D, Adroja D T, Bhattacharyya A, Hillier A D, Manuel P, Strydom A M, Kawabata J and Takabatake T 2014 *Phys. Rev. B* **89** 064422
[12] Bhattacharyya A, Adroja D T, Strydom A M, Kawabata J, Takabatake T, Hillier A D, Sakai V G, Taylor J W and Smith R I 2014 *Phys. Rev. B* **90** 174422
[13] Ekino T, Takabatake T, Tanaka H and Fujii H 1995 *Phys. Rev. Let.* **75** 4262
[14] Wolf E L 2012 *Principles of Electron Tunneling Spectroscopy*, 2nd ed. (New York: Oxford University Press).
[15] Flachbart K, Gloos K, Konovalova E, Paderno Y, Reiffers M, Samuely P and Svec P 2001 *Phys. Rev. B* **64** 085104
[16] Riseborough P S and Magalhaes S G 2016 *J. Magn. Magn. Mat.* **400** 3
[17] Motoyama G, Ogawa S, Matsubayashi K, Fujiwara K, Miyoshi K, Nishigori S, Mutou T, Yamaguchi A, Sumiyama A and Uwatoko Y 2015 *Phys. Proc.* **75** 296
[18] Kimura S, Iizuka T, Miyazaki H, Irizawa A, Muro Y and Takabatake T 2011 *Phys. Rev. Lett.* **106** 056404
[19] Yamada Y, Kawabata J, Onimaru T and Takabatake T 2015 *J. Phys. Soc. Jpn.* **84** 084705